HAL open science

Static limit analysis and strength of porous solids with hill orthotropic matrix

I. El Ghezal, I. Doghri, D. Kondo

▶ To cite this version:

I. El Ghezal, I. Doghri, D. Kondo. Static limit analysis and strength of porous solids with hill orthotropic matrix. International Journal of Solids and Structures, 2017, 109, pp.63 - 71. 10.1016/j.ijsolstr.2017.01.007 . hal-01472156

HAL Id: hal-01472156

https://hal.sorbonne-universite.fr/hal-01472156

Submitted on 20 Feb 2017

HAL is a multi-disciplinary open access archive for the deposit and dissemination of scientific research documents, whether they are published or not. The documents may come from teaching and research institutions in France or abroad, or from public or private research centers.

L'archive ouverte pluridisciplinaire HAL, est destinée au dépôt et à la diffusion de documents scientifiques de niveau recherche, publiés ou non, émanant des établissements d'enseignement et de recherche français ou étrangers, des laboratoires publics ou privés.

Static Limit Analysis and strength of porous solids with Hill orthotropic matrix

M. I. El Ghezal[a,*], I. Doghri[a], D. Kondo[b]

[a] *Université catholique de Louvain (UCL), iMMC, Bâtiment Euler, 4 Avenue G.Lemaître B-1348 Louvain-La-Neuve, Belgium*
[b] *Université Pierre et Marie-Curie, Institut Jean Le Rond d'Alembert, 4 place de Jussieu F75005 Paris, France*

Abstract

The present study deals with a strength criterion for ductile porous materials consisting in a Hill type orthotropic matrix containing spherical voids. The originality of the study lies into an attempt to develop an approximate static Limit Analysis for this class of materials, based on the recent work of Cheng et al. (2014) initially proposed for isotropic von Mises matrix. To this end, we considered, in the framework of a statical limit analysis framework, a trial stress field complying with the boundary conditions of the homogenization problem. Interestingly, the proposed procedure delivers an anisotropic macroscopic criterion which is not only pressure dependent, but exhibits an original sensitivity to the sign of the third invariant of the stress deviator. The obtained results are discussed and compared to existing theoretical models, to numerical bounds and to recently available Finite Element results. Finally, we provide the plastic strain rate equations and the void evolution law which are crucial for formulating the failure of anisotropic ductile metals. The influence of the plastic anisotropy on these constitutive equations is illustrated.

Keywords: Ductile porous materials; Hill orthotropic matrix; Statical limit

*Corresponding author.Tel: +32-10-472362/472350; fax: +32-10-472180.
Email address: marieme.elghezal@uclouvain.be (M. I. El Ghezal)

analysis; Third stress invariant.

Introduction

The macroscopic yielding and plastic behavior of isotropic porous materials have been extensively studied following the pioneering kinematical approach proposed by Gurson [19] who studied a hollow sphere and a hollow cylinder subjected to uniform strain rate boundary conditions. The considered matrix is made up of a rigid-perfectly plastic material obeying the von Mises criterion. Although Gurson's kinematical analysis involves several approximations, it has been shown later that the obtained result preserves the upper bound character of the macroscopic criterion (see for instance [39]).

Still in the context of Kinematic Limit Analysis[1], the standard Gurson model was later extended by Tvergaard [43] and subsequently by Perrin and Leblond [40] in a theoretical approach by introducing additional parameters in order to better fit finite element (FE) unit cell computations and to account for the interaction between voids [2]. Other extensions accounting for void shape effects were further developed for spheroidal voids (e.g. prolate and oblate ellipsoidal cavities) by [29] and [30], [17], [16] and then [33]. Pardoen and Hutchinson [36] integrated the extended model of Gologanu-Leblond-Devaux [17] into a heuristically enhanced void growth and coalescence model incorporating the effect of strain hardening. Studies concerning pressure-sensitive dilatant matrix have been also proposed by [18] (see also[9], [11], [26] and [25]) who used a Drucker-Prager yield criterion to describe the compressibility of the matrix.

---

[1]Another class of models for porous materials has been proposed in the literature based on variational non linear homogenization techniques (see for instance [5], [6], [13] and [12]).

[2]Note also the well-known computational results of Koplik and Needleman [24].

All the above mentioned extensions concern an isotropic matrix. However, initial anisotropy may be either naturally present in various engineering materials or induced by the deformation during forming processes (e.g rolling, drawing and extrusion). That has motivated several studies dealing with ductile porous materials with plastically anisotropic matrix. Indeed, Benzerga and Besson [4] extended the Gurson yield criterion to porous materials with Hill orthotropic matrix. This model has been extended by Monchiet et al. [32] and then by Keralavarma and Benzerga [27] who developed micromechanical models that couple both the matrix anisotropy and void shape effects by considering spheroidal voids. Recently, Morin et al.[35] evaluated the above mentioned criteria using a new FE technique for numerical limit-analysis of Hill materials. Their method is based on the standard FE method. More completely, Pastor et al. [38] provided numerical upper and lower bounds for the macroscopic criteria of orthotropic plastic materials using static and kinematic numerical limit analysis codes. The case of a Hill type matrix with arbitrary ellipsoidal voids has been very recently investigated by [34]. All the above models with matrix anisotropy have been derived from a kinematic limit analysis approach (except the numerical static bound of Pastor et al.) and thus yield upper bounds of the macroscopic yield criterion. Recently, Cheng et al. [8] proposed an original statical limit analysis procedure for porous materials with isotropic von Mises solid matrix. Notable feature of the static-based model is the prediction of the third invariant in a rather easy way [3]. The ease of the derivation of the macroscopic criterion and the validity of the results obtained using this approach make it an attractive alternative to kinematics-based models.

In the present study, we are concerned with the anisotropic plastic behavior

[3]This work has been preceded by that performed in the context of kinematical approach of Limit Analysis by Cazacu et al [7] who had investigated the effect of the sign of the third invariant for a von Mises matrix.

of ductile porous metals and provide a static-based limit analysis of a Hill-type anisotropic matrix containing spherical voids. This will lead to a fully explicit macroscopic criterion. The plastic strain rate equations and the void evolution law which are crucial for formulating the anisotropic plastic behavior of ductile porous metals will be also provided.

The outline of the paper is as follows: The static limit analysis recently proposed by Cheng et al.[8] is first briefly recalled in section 1. In section 2, an approximate criterion is developed by applying the statical approach to materials with anisotropic matrix and considering a new appropriate trial stress field. The obtained criterion is illustrated in section 3, while a comparison of the model predictions with those obtained from FE computations on unit cells (see [35]) is presented. Numerical upper and lower bounds established by [38] are also considered for this comparison purpose. Finally, in section 5, we provide the void growth equations and illustrate the porosity evolution laws for different examples of materials anisotropy.

1. Basic principles of the static limit analysis approach of porous materials

In this section, general features of the statical limit analysis [4] of porous media presented by Cheng et al. [8] are briefly recalled in the perspective of the extension that we will expose below for ductile materials with anisotropic matrix.

Scale transition from microscopic scale (typical size of a cavity) to the macroscopic one is performed in the context of standard uniform boundary conditions. The macroscopic stress $\mathbf{\Sigma}$ and strain rate $\mathbf{D}$ are then obtained from the volume averages of their microscopic counterparts $\boldsymbol{\sigma}$ and $\mathbf{d}$ over the considered Representative

[4] A thorough overview of the theory of limit analysis can be found in [3] and [42]

Volume Element (RVE) of the porous material:

$$\mathbf{\Sigma} = \frac{1}{|\Omega|}\int_{\Omega-\omega} \boldsymbol{\sigma}\, dV, \quad \mathbf{D} = \frac{1}{|\Omega|}\int_{\Omega} \mathbf{d}\, dV \tag{1}$$

Ω refers to the domain occupied by the RVE, while $\Omega - \omega$ corresponds to that of the solid matrix.

Let us introduce the set $\kappa(V(x))$ of kinematically and plastically admissible and incompressible velocity fields:

$$\kappa(\mathbf{V}(x)) = \{\mathbf{V}(x) = \mathbf{D}.\mathbf{x} \text{ on } \partial\Omega \text{ and } d_{kk} = 0 \text{ with } \mathbf{d} = \frac{1}{2}(\nabla(\mathbf{V}) + \nabla^T(\mathbf{V}))\} \tag{2}$$

The set $\chi(\boldsymbol{\sigma})$ of statically admissible stress fields is given by:

$$\chi(\boldsymbol{\sigma}) = \{\boldsymbol{\sigma},\ \sigma_{ij} = \sigma_{ji},\ \text{div}\, \boldsymbol{\sigma} = 0,\ \boldsymbol{\sigma}.\mathbf{n} = 0 \text{ on } \partial\omega\} \tag{3}$$

Let us recall the Hill-Mandel Lemma ([22]) which states that the macroscopic work rate equals the average microscopic one and reads as follows:

$$\mathbf{\Sigma} : \mathbf{D} = \frac{1}{|\Omega|}\int_{\Omega-\omega} \boldsymbol{\sigma} : \mathbf{d}\, dV \tag{4}$$

in which $(\mathbf{V}, \boldsymbol{\sigma})$ is an admissible couple. Moreover, the principle of maximum plastic work, introduced by Hill [21], states that:

$$\forall \boldsymbol{\sigma}^* \in C,\ (\boldsymbol{\sigma}^* - \boldsymbol{\sigma}) : \mathbf{d} \leq 0, \tag{5}$$

where C is the convex set of plastic admissible stress fields (defined by the criterion $f(\boldsymbol{\sigma}) \leq 0$ where f is the considered yield function). Introducing the indicator function $\psi(\boldsymbol{\sigma})$ of the plastic domain, defined by:

$$\begin{cases} \psi(\boldsymbol{\sigma}) = 0 \Leftrightarrow \ \boldsymbol{\sigma} \in C \\ \psi(\boldsymbol{\sigma}) = +\infty \ \Leftrightarrow \ \boldsymbol{\sigma} \notin C \end{cases}, \tag{6}$$

the inequality (5) is reexpressed as:

$$\mathbf{d} \in \partial\psi(\boldsymbol{\sigma}) \tag{7}$$

where $\partial\psi(\boldsymbol{\sigma})$ is the subdifferential of ψ. Hill's variational principle [21] states that among the stress fields, the true one makes the functional:

$$\int_{\Omega-\omega} \psi(\boldsymbol{\sigma})dV - \int_{\Gamma_{\mathbf{V}}} (\boldsymbol{\sigma}.\mathbf{n}).\mathbf{V}\, ds \tag{8}$$

an absolute minimum. In (8), $\mathbf{V}$ denotes the prescribed velocity on a part $\Gamma_{\mathbf{V}}$ of the boundary of the cell. An average functional Φ over the RVE, appropriate for the homogenization problem, is introduced such that:

$$\Phi = \min_{\sigma\in\chi(\sigma)} \left(\frac{1}{|\Omega|}\int_{\Omega-\omega} \psi(\boldsymbol{\sigma})\, dV - \boldsymbol{\Sigma} : \mathbf{D}\right) \tag{9}$$

Since $\psi(\boldsymbol{\sigma})$ vanishes for licit $\boldsymbol{\sigma}$, this variational problem is equivalent to the following one:

$$\min_{\sigma\in\chi_l(\sigma)} (-\boldsymbol{\Sigma} : \mathbf{D}), \tag{10}$$

where:

$$\chi_l(\boldsymbol{\sigma}) = \{\boldsymbol{\sigma} \in \chi(\boldsymbol{\sigma}),\ \ f(\boldsymbol{\sigma}) \leq 0\}, \tag{11}$$

The resulting minimization problem is solved using Lagrangian functional. By relaxing the yield criterion [5] and imposing the Lagrange multiplier to be uniform over the matrix, the resulting saddle-point problem takes the following simple form:

$$\max_{\dot{\lambda}\geq 0}\min_{\sigma\in\chi_l(\sigma)} \left(L(\boldsymbol{\sigma},\dot{\lambda}) = \dot{\lambda}\frac{1}{|\Omega|}\int_{\Omega-\omega} f(\boldsymbol{\sigma})\,dV - \boldsymbol{\Sigma} : \mathbf{D}\right) \tag{12}$$

The considered static limit analysis approach results into a stress variational model which is equivalent to minimizing the functional Φ under the condition:

$$F(\boldsymbol{\Sigma}) = \frac{1}{|\Omega|}\int_{\Omega-\omega} f(\boldsymbol{\sigma})\,dV = 0 \tag{13}$$

This equality condition on $\boldsymbol{\Sigma}$ is interpreted as the equation of the macroscopic yield function.

The crucial step to obtain $F(\boldsymbol{\Sigma})$ consists in finding a trial stress field $\boldsymbol{\sigma}$ satisfying both the equilibrium equations and the void boundary conditions and implementing it into (13). Once $F(\boldsymbol{\Sigma})$ determined, the macroscopic flow rule is obtained by performing the derivation of the Lagrangian functional $L(\sigma,\dot{\lambda})$ with respect to $\boldsymbol{\Sigma}$. This reads:

$$\mathbf{D} = \dot{\lambda}\frac{\partial F}{\partial \boldsymbol{\Sigma}}, \quad \dot{\lambda} \geq 0 \tag{14}$$

where $\dot{\lambda}$ can be interpreted as a plastic multiplier.

2. Formulation of the approximate yield criterion

2.1. The general procedure

Let us now consider as a cell corresponding to the RVE a hollow sphere having external and internal radii b and a, respectively such that the void volume fraction p (porosity) reads $p = (\frac{a}{b})^3$. This hollow sphere is subjected to linear velocities on

[5] Following the numerical works of Nguyen [14], the yield criterion is satisfied only in an average sense.

($r = b$) corresponding to a uniform strain rate. The solid matrix material is assumed to be rigid-perfectly plastic and obeying Hill's [20] quadratic orthotropic criterion. With respect to a Cartesian coordinate system that coincides with the symmetry axes of the plastic anisotropic matrix, the criterion is classically expressed as:

$$f(\boldsymbol{\sigma}) = \sigma_e - \sigma_0 = \sqrt{\frac{3}{2}\,\boldsymbol{\sigma} : \mathbf{M} : \boldsymbol{\sigma}} - \sigma_0 \leq 0 \tag{15}$$

where σ_0 is the yield stress of the material in a reference direction and $\mathbf{M}$ is a symmetric fourth-order orthotropy tensor ($M_{ijkl} = M_{jikl} = M_{ijlk}$). With respect to the symmetry axes, the fourth-order tensor $\mathbf{M}$ takes the following form in the standard Voigt notation (6×6 matrix), the stress tensor being given as a vector:

$$\mathbf{M} = \begin{bmatrix} H+G & -H & -G & 0 & 0 & 0 \\ -H & F+H & -F & 0 & 0 & 0 \\ -G & -F & F+G & 0 & 0 & 0 \\ 0 & 0 & 0 & 2L & 0 & 0 \\ 0 & 0 & 0 & 0 & 2M & 0 \\ 0 & 0 & 0 & 0 & 0 & 2N \end{bmatrix}; \quad \boldsymbol{\sigma} = \begin{bmatrix} \sigma_{11} \\ \sigma_{22} \\ \sigma_{33} \\ \sigma_{23} \\ \sigma_{13} \\ \sigma_{12} \end{bmatrix} \tag{16}$$

Note that the Hill criterion reduces to the isotropic von Mises one when the characteristic constants read $F = G = H = 1/3$ and $L = M = N = 1$.

For the tractability of the determination of $F(\sigma)$ from (13), and similarly to the choice made by [4] and then Monchiet et al. [32] in the context of kinematic limit analysis, we will consider an isotropic trial stress field:

$$\boldsymbol{\sigma} = \boldsymbol{\sigma}^{(1)} + \boldsymbol{\sigma}^{(2)}, \tag{17}$$

where $\boldsymbol{\sigma}^{(1)}$ reads in spherical coordinates ($r, \theta \in [0, \pi], \phi \in [0, 2\pi]$):

$$\boldsymbol{\sigma}^{(1)} = -C_0 \left(\ln(\frac{a}{r})\mathbf{1} - \frac{1}{2}(\mathbf{e}_\theta \otimes \mathbf{e}_\theta + \mathbf{e}_\phi \otimes \mathbf{e}_\phi)\right), \tag{18}$$

C_0 is a constant to be determined and $\mathbf{1}$ denotes the second order identity tensor. $\boldsymbol{\sigma}^{(1)}$ corresponds to the exact stress field in the case of hydrostatic loading for an isotropic matrix. The second part $\boldsymbol{\sigma}^{(2)}$ is taken for capturing the shear stress effects. At the difference of [8] who consider an homogeneous stress field, $\boldsymbol{\sigma}^{(2)}$ is inspired here from the exact solution to linear elastic hollow sphere problem subjected to deviatoric loading (see [23])[6]:

$$\begin{aligned}
\sigma_{rr}^{(2)} &= [3\nu A_1 x^2 + A_2 - 2(5-\nu)A_3 x^{-3} - 12A_4 x^{-5}](1 + 3\cos 2\theta), \\
\sigma_{\theta\theta}^{(2)} &= \begin{matrix}[7(2+\nu)A_1 x^2 - A_2 + (1-2\nu)A_3 x^{-3} + 7A_4 x^{-5}](1+3\cos 2\theta) \\ + [-2(7-4\nu)A_1 x^2 + 2A_2 + 4(1-2\nu)A_3 x^{-3} - 4A_4 x^{-5}]\end{matrix}, \\
\sigma_{\phi\phi}^{(2)} &= \begin{matrix}[(7+11\nu)A_1 x^2 + 3(1-2\nu)A_3 x^{-3} + 5A_4 x^{-5}](1+3\cos 2\theta) \\ + [2(7-4\nu)A_1 x^2 - 2A_2 - 4(1-2\nu)A_3 x^{-3} + 4A_4 x^{-5}]\end{matrix}, \\
\sigma_{r\theta}^{(2)} &= 3[(7+2\nu)A_1 x^2 - A_2 - 2(1+\nu)A_3 x^{-3} - 8A_4 x^{-5}]\sin 2\theta
\end{aligned} \tag{19}$$

in spherical coordinates. Where:

$$\begin{aligned}
A_1 &= 5(p^{-5/3} - p^{-1})C_1/\Delta, \\
A_2 &= [(49 - 25\nu^2)p^{-10/3} + 126p^{-5/3} + 25(\nu^2 - 7)p^{-1}]C_1/6\Delta, \\
A_3 &= 5(7+5\nu)(p^{-10/3} - p^{-1})C_1/12\Delta, \\
A_4 &= -(7+5\nu)(p^{-10/3} - p^{-5/3})C_1/4\Delta
\end{aligned} \tag{20}$$

and $\Delta = [(49-25\nu^2)p^{-10/3} + 25(\nu^2-7)p^{-7/3} + 252p^{-5/3} + 25(\nu^2-7)p^{-1} + (49-25\nu^2)]$.

[6] *This idea is similar to that already used by [15] in the context of kinematics limit analysis of isotropic porous materials.*

C_1 is also a constant parameter, $x = \frac{r}{a}$ and ν is a free parameter which must be determined by minimizing the macroscopic potential. [7]

In contrast to the homogeneous deviatoric part taken in [8], the considered stress field $\boldsymbol{\sigma}^{(2)}$ satisfies not only the equilibrium equations but also the boundary conditions on the inner surface of the hollow sphere.

The microscopic equivalent stress in the matrix $\sigma_e = \sqrt{\frac{3}{2}\boldsymbol{\sigma} : \mathbf{M} : \boldsymbol{\sigma}}$ is computed in a straightforward manner and is found to be a function of both r,θ and ϕ that could be recast in the form:

$$\sigma_e = \sqrt{C_0^2 f_1(r,\theta,\phi) + C_1^2 f_2(r,\theta,\phi) + C_0 C_1 f_3(r,\theta,\phi)}, \tag{21}$$

where f_1, f_2 and f_3 are combinations of functions of r, θ and ϕ, whose expressions are long so they were omitted here for brevity. The computation of the axisymmetric macroscopic stress tensor using (1) yields:

$$\boldsymbol{\Sigma} = -\frac{C_0 \ln p}{3}\mathbf{1} - \frac{1}{3}C_1(\mathbf{e}_1 \otimes \mathbf{e}_1 + \mathbf{e}_2 \otimes \mathbf{e}_2 - 2\mathbf{e}_3 \otimes \mathbf{e}_3) \tag{22}$$

It follows that the macroscopic mean stress Σ_m, the macroscopic Hill equivalent stress Σ_e and the third invariant of the deviatoric part $\mathbf{S}$ of $\boldsymbol{\Sigma}$, noted J_3, are given by:

$$\Sigma_m = -\frac{C_0 \ln p}{3}, \quad \Sigma_e^2 = \frac{3}{2}\boldsymbol{\Sigma} : \mathbf{M} : \boldsymbol{\Sigma} = \frac{3}{2}(F+G)C_1^2, \quad J_3 = \frac{tr(\mathbf{S}^3)}{3} = \frac{2}{27}C_1^3 \tag{23}$$

Note that in equation (23), the macroscopic Hill equivalent stress Σ_e depends only on coefficients F and G through their sum $F+G$. This is due to the axisymmetric

[7] Note that ν (which may not be interpreted here as an elastic coefficient) has been shown by optimization of $F = \frac{1}{|\Omega|}\int_{\Omega-\omega} f(\sigma)\, dV$ to be equal to 0.5

character of the considered loadings. Anticipating on developments which will follow, we introduce the following alternative expressions [8]:

$$\tilde{\Sigma}_e = \frac{\Sigma_e}{\sqrt{\frac{3}{2}(F+G)}} = |C_1| \;\; , \;\; \tilde{\Sigma}_m = -\frac{3\Sigma_m}{\ln p} = C_0 \;\; , \;\; \text{sign}(J_3) = \frac{27}{2}\frac{J_3}{\tilde{\Sigma}_e^{\,3}} = \text{sign}(C_1) \quad (24)$$

According to (13), the macroscopic yield surface is defined by:

$$F(\mathbf{\Sigma}) = \frac{1}{|\Omega|}\int_{\Omega-\omega} \sigma_e(r,\theta,\phi)\, r^2 \sin\theta \, d\theta \, d\phi \, dr - (1-p)\,\sigma_0 \quad (25)$$

where, taking into account (24), the microscopic equivalent stress (eq. 21) , can be recast in the form:

$$\begin{aligned} \sigma_e = & \sqrt{f_1(r,\theta,\phi)\tilde{\Sigma}_m^2 + f_2(r,\theta,\phi)\tilde{\Sigma}_e^2 + f_3(r,\theta,\phi) sign(J_3)\tilde{\Sigma}_m\tilde{\Sigma}_e} \\ = & \sqrt{f_1(r,\theta,\phi)\frac{9\Sigma_m^2}{\ln^2 p} + f_2(r,\theta,\phi)\frac{\Sigma_e^2}{3/2(F+G)} - f_3(r,\theta,\phi) sign(J_3)\frac{\Sigma_e}{\sqrt{3/2(F+G)}}\frac{3\Sigma_m}{\ln p}} \end{aligned} \quad (26)$$

Due to presence of the functions f_1,f_2 and $f_3(r,\theta,\phi)$, a closed form expression of the macroscopic criterion $F(\mathbf{\Sigma})$ by combining (25) and (26) is out of reach; this has motivated the approximations described below.

2.2. *Approximate criterion based on Cauchy-Schwarz inequality*

A first approximation of the macroscopic criterion can be obtained by adopting the Cauchy-Schwarz inequality, as in several previous works including those on porous materials with Hill orthotropic matrix (see for instance Benzerga et al. [4]

[8]Note that if Z is the tensile yield stress in the principal anisotropy direction z, then we have $F+G=\frac{1}{Z^2}$ which confirms the positiveness of $F+G$ and allows its use in the square root.

or [32]). This easies the computation of the integral in (25) and leads to:

$$\frac{1}{|\Omega|}\int_{\Omega-\omega}\sigma_e(r,\theta,\phi)r^2 sin\theta d\theta d\phi dr-(1-p)\sigma_0 \leq \frac{1}{|\Omega|}\sqrt{|\Omega-\omega|\int_{\Omega-\omega}\sigma_e^2(r,\theta,\phi)\, r^2 sin\theta\, d\theta\, d\phi\, dr}-(1-p)\sigma_0 \tag{27}$$

The macroscopic criterion is obtained in the form:

$$\sqrt{\alpha\tilde{\Sigma}_e^2+\beta\tilde{\Sigma}_m^2+\gamma sign(J_3)\tilde{\Sigma}_e\tilde{\Sigma}_m}-\sigma_0 \leq 0, \tag{28}$$

where α, β and γ are combinations of both the matrix anisotropy characteristics and the porosity p. A power series expansion of those quantities up to order 1 allows to get a simplified expression:

$$\begin{aligned}
&\alpha = \tfrac{3}{2}(F+G)+[\tfrac{631}{189}(F+G)+\tfrac{40}{189}H+\tfrac{20}{189}N+\tfrac{25}{189}(L+M)]p+O(p^2),\\
&\beta = \tfrac{1}{20}[2(F+G+H)+L+M+N],\\
&\gamma = \tfrac{1}{21}[-(L+M)-2(G+F-N)+4H]p\ln p+(p-p^{\frac{5}{3}})[\tfrac{-32}{95}H+\tfrac{8}{95}(L+M)+\tfrac{16}{95}(F+G-N)]+O(p^2).
\end{aligned} \tag{29}$$

which proved to be a good approximation of the exact expression for porosity values up to 0.15. The new criterion takes the following form:

$$\sqrt{\frac{\alpha}{\frac{3}{2}(F+G)}(\frac{\Sigma_e}{\sigma_0})^2+\frac{9}{(\ln p)^2}\beta\,(\frac{\Sigma_m}{\sigma_0})^2-\frac{3\gamma sign(J_3)}{\sqrt{\frac{3}{2}(F+G)}\ln p}\frac{\Sigma_e}{\sigma_0}\frac{\Sigma_m}{\sigma_0}}-1\leq 0 \tag{30}$$

In the limit of a vanishing porosity, one can check that since $\ln\, p \rightarrow -\infty$ and $\alpha \rightarrow \frac{3}{2}(F+G)$, the Hill quadratic criterion of the matrix is obviously retrieved. Interestingly, criterion (30) shows an influence of the sign of the third deviatoric stress invariant. Such type of effect has been already pointed out in a recent kinematic-based limit analysis study by [7] for von Mises matrix materials (see also [1] or [41] for the effect of Lode angle) and by [8] in the context of the static approach (this result has been recently extended to the influence of Lode angle

[10]). An originality of the present result is that the effect of the sign of the third deviatoric stress invariant is coupled with the matrix anisotropy. In the limit of isotropic matrix, the criterion reduces to:

$$\sqrt{(1+\frac{8}{3}p)(\frac{\Sigma_e}{\sigma_0})^2+\frac{9}{4(\ln p)^2}(\frac{\Sigma_m}{\sigma_0})^2}-1\leq 0 \tag{31}$$

Remark1: The obtained criterion (31) has the same shape as the approximate one obtained by [8] but differs from it by the factor multiplying Σ_e. Indeed, in the approximate criterion of Cheng et al. [8] the pure deviatoric point corresponds to $\frac{\Sigma_e}{\sigma_0}=1-p$, which is the same as in the Gurson model and which corresponds to Voigt upper bound. This difference is obviously due to the choice of the trial stress field, the one considered here being more refined.

Remark2: It should be pointed out that for hydrostatic macroscopic stresses, as expected, the isotropic criterion (31) predicts the same yield loci as in Gurson model and Cheng et al. [8] and which corresponds to the exact solution of porous materials with a von Mises matrix: $\frac{\Sigma_m}{\sigma_0}=-\frac{2}{3}\ln p$. The pure deviatoric point corresponds to $\frac{\Sigma_e}{\sigma_0}=\frac{1}{\sqrt{1+\frac{8}{3}p}}$ which is, for $p\leq 0.15$, bounded below by the deviatoric point given by the elliptic criteria of [5] and [31] (which correspond to $\frac{\Sigma_e}{\sigma_0}=\frac{1-p}{\sqrt{1+\frac{2}{3}p}}$) and bounded above by the one given by Gurson and Cheng et al.[8].

Remark3: It can be noted that in the isotropic case, the effect of the third deviatoric stress disappears, this is due to the vanishing value of γ. This absence of the third stress deviator invariant contrasts with , the result established by [8] in the context of static limit analysis. This limitation may be obviously attributed to the use of the Cauchy-Schwarz inequality and has motivated an alternative approach presented in what follows.

2.3. Approximate criterion based on Taylor series expansion

Indeed, the microscopic equivalent stress σ_e may be put in the following form:

$$\sigma_e = \sqrt{f_1(r,\theta,\phi)\tilde{\Sigma}_m^2 + f_2(r,\theta,\phi)\tilde{\Sigma}_e^2}\,\sqrt{1+\varrho(r,\theta,\phi)} \tag{32}$$

where

$$\varrho(r,\theta,\phi) = \frac{f_3(r,\theta,\phi)sign(J_3)\tilde{\Sigma}_m\tilde{\Sigma}_e}{f_1(r,\theta,\phi)\tilde{\Sigma}_m^2 + f_2(r,\theta,\phi)\tilde{\Sigma}_e^2}$$

Assuming $\varrho(r,\theta,\phi)$ to be small, we adopt here an alternative approximation consisting in performing a Taylor series expansion of the expression $\sqrt{1+\varrho(r,\theta,\phi)}$ involved in (32) [9]:

$$\begin{aligned}\sigma_e \;\approx\; & \sqrt{<f_1>_{\Omega-\omega}\tilde{\Sigma}_m^2 + <f_2>_{\Omega-\omega}\tilde{\Sigma}_e^2}\,\Bigg[1+\frac{1}{2}\,\frac{f_3(r,\theta,\phi)sign(J_3)\tilde{\Sigma}_m\tilde{\Sigma}_e}{<f_1>_{\Omega-\omega}\tilde{\Sigma}_m^2 + <f_2>_{\Omega-\omega}\tilde{\Sigma}_e^2}\\ & -\frac{1}{8}\,\frac{f_3(r,\theta,\phi)^2\tilde{\Sigma}_m^2\tilde{\Sigma}_e^2}{(<f_1>_{\Omega-\omega}\tilde{\Sigma}_m^2 + <f_2>_{\Omega-\omega}\tilde{\Sigma}_e^2)^2} + \frac{1}{16}\,\frac{f_3(r,\theta,\phi)^3 sign(J_3)\tilde{\Sigma}_m^3\tilde{\Sigma}_e^3}{(<f_1>_{\Omega-\omega}\tilde{\Sigma}_m^2 + <f_2>_{\Omega-\omega}\tilde{\Sigma}_e^2)^3}\Bigg]\end{aligned} \tag{33}$$

for which has been made a complementary approximation consisting in replacing $f_1(r,\theta,\phi)$ and $f_2(r,\theta,\phi)$ by their mean values in the matrix $<f_1>_{\Omega-\omega}$ and $<f_2>_{\Omega-\omega}$, respectively. One gets:

$$<f_1>_{\Omega-\omega} = \frac{1}{|\Omega-\omega|}\int_{\Omega-\omega} f_1 d\mathrm{v} = \beta\;;\; <f_2>_{\Omega-\omega} = \frac{1}{|\Omega-\omega|}\int_{\Omega-\omega} f_2 d\mathrm{v} = \alpha \tag{34}$$

The determination of the macroscopic criterion requires also the following integrations:

$$\begin{aligned}&\tfrac{1}{|\Omega-\omega|}\int_{\Omega-\omega} f_3 d\mathrm{v} = \gamma\\ &\tfrac{1}{|\Omega-\omega|}\int_{\Omega-\omega} f_3^2 d\mathrm{v} = \xi\\ &\tfrac{1}{|\Omega-\omega|}\int_{\Omega-\omega} f_3^3 d\mathrm{v} = \chi\end{aligned} \tag{35}$$

[9] *This follows an idea already implemented in the isotropic case by [28] who has revisited the Gurson kinematic limit analysis.*

Let us draw the attention to the fact that α, β and γ are given by (29). The expressions of ξ and χ, which are functions of anisotropy parameters and porosity p are obtained as:

$$\begin{aligned}\xi &= \tfrac{3}{5}(F^2 + G^2 + FG),\\ \chi &= \frac{27}{640}\frac{(-32 - 323\pi)G^3 + (685\pi - 536)F^3 + (11\pi - 224)F^2G - (373\pi + 32)G^2F}{\pi}.\end{aligned} \tag{36}$$

Finally, introducing (33), (34) and (35) into (25) yields the following general form of the macroscopic criterion:

$$\sqrt{\alpha\tilde{\Sigma}_e^2 + \beta\tilde{\Sigma}_m^2}\left[1+\frac{\gamma}{2}\frac{sign(J_3)\tilde{\Sigma}_m\tilde{\Sigma}_e}{\alpha\tilde{\Sigma}_e^2 + \beta\tilde{\Sigma}_m^2}-\frac{\xi}{8}\frac{\tilde{\Sigma}_m^2\tilde{\Sigma}_e^2}{(\alpha\tilde{\Sigma}_e^2 + \beta\tilde{\Sigma}_m^2)^2}+\frac{\chi}{16}\frac{sign(J_3)\tilde{\Sigma}_m^3\tilde{\Sigma}_e^3}{(\alpha\tilde{\Sigma}_e^2 + \beta\tilde{\Sigma}_m^2)^3}\right]-\sigma_0 \leqslant 0 \tag{37}$$

for which it is recalled that $\tilde{\Sigma}_m$ and $\tilde{\Sigma}_e$ are defined in (24).

Note that (37) obviously reduces to the Hill quadratic criterion (of the matrix) in the limit $p \longrightarrow 0$.

It is worth noticing that in the particular case of the von Mises isotropic matrix, the parameter χ does not vanish and thus an effect of the third invariant in that case is obtained:

$$\sqrt{(1 + \frac{8}{3}p)(\frac{\Sigma_e}{\sigma_0})^2 + \frac{9}{4(\ln p)^2}\,(\frac{\Sigma_m}{\sigma_0})^2}\;\Pi(sign(J_3), T, p) - 1 \leq 0, \tag{38}$$

with

$$\Pi(sign(J_3), T, p) = \left[1-\frac{1}{8}\frac{1}{5}\left(\frac{\frac{-3T}{\ln p}}{(1 + \frac{8}{3}p) + \frac{9}{4(\ln p)^2}T^2}\right)^2-\frac{1}{16}\frac{103}{80\pi}sign(J_3)\left(\frac{\frac{-3T}{\ln p}}{(1 + \frac{8}{3}p) + \frac{9}{4(\ln p)^2}T^2}\right)^3\right] \tag{39}$$

and T denotes the stress triaxiality $T = \Sigma_m/\Sigma_e$.

Remark 4: The criterion takes the same shape as in [8]. Besides, the function

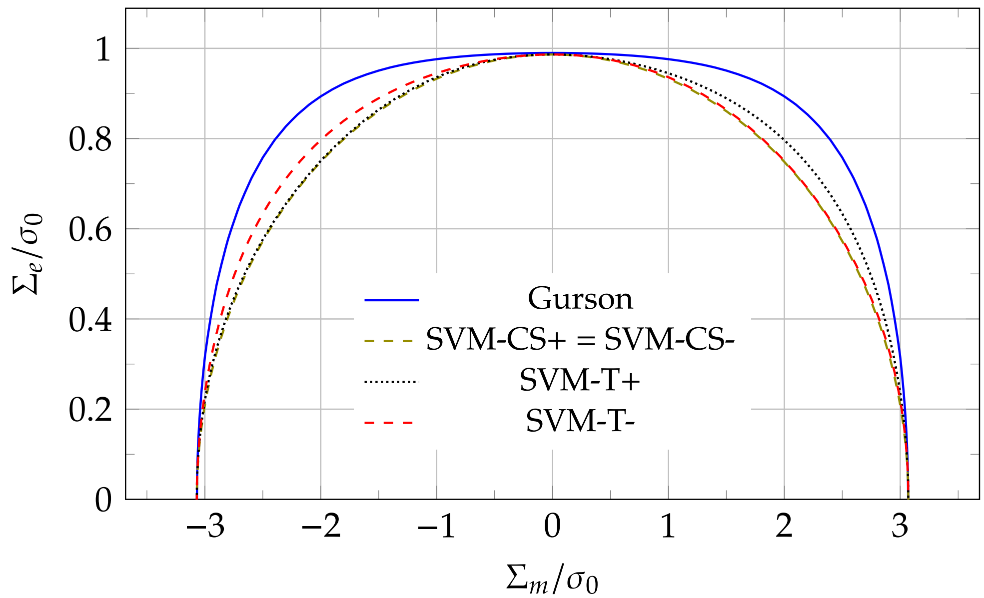

Figure 1: Yield surfaces of a metal matrix porous solid with 1% porosity given respectively by Gurson [19] and by the proposed new criteria. Acronyms SVM-CS+ and SVM-CS- refer respectively to criterion (31) for $J_3 > 0$ and for $J_3 < 0$ and acronyms , SVM-T+ and SVM-T- refer respectively to criterion (38) for $J_3 > 0$ and for $J_3 < 0$.

$\Pi(sign(J_3), T, p)$ is smooth for $p \in [0, 1]$ and $T \in]-\infty, +\infty[$ and takes values between 0.949 and 1.050; thus, as in [8], one can obtain an approximate criterion by taking $\Pi(sign(J_3), T, p)$ to be unity. However, it should be pointed out that in that case the influence of the third invariant J_3 is lost. Remarks 1-2 remain valid for this second criterion.

3. Illustration of the established macroscopic criterion

In this section, we aim at illustrating some salient features of the obtained criteria. The yield curve corresponding to the new criteria in the isotropic case and its comparison with Gurson model for a porosity p=0.01 are reported on Fig 1.

It is seen that the yield envelopes predicted by the new criteria stay inside the Gurson kinematic one as expected. It is recalled that for the isotropic case, the parameter γ vanishes and thus there is no effect of (J_3) predicted by the criterion

Table 1: Hill's coefficients considered for the different studied cases

Material's parameters	F	G	H	L	M	N
Isotropic: Fig 1	1/3	1/3	1/3	1	1	1
Set 1: Fig 2, Fig 8	0.332	0.332	0.999	1	1	2.333
Set 2: Fig 3, Fig 6	0.268	0.345	0.311	1.096	3.622	3.498
Set 3: Fig 4, Fig 7	0.331	0.402	0.168	3.669	1.141	2.2

(30) named SVM-CS. However, this effect is still present for the criterion obtained by Taylor series expansion (37) named SVM-T.

Let us consider now the anisotropic case for which the parameters chosen for every figure are indicated in table 1. In Figures 2(a) and 2(b) we compare the yield curves predicted by the new criteria (30) and (37) for $J_3 > 0$ and $J_3 < 0$ to those pertaining to Benzerga et al. [4] model; two porosity values, $p = 0.01$ and $p = 0.1$ are considered. It is observed that the obtained criteria display an asymmetry with respect to the axis $\Sigma_m = 0$ due to the sign of J_3. A zoom on appropriate portions of the figure reveals that the predicted macroscopic yield surface obtained by the Cauchy-Schwarz inequality (30) is within the one obtained by Taylor series expansion (37) and the effect of $sign(J_3)$ is more pronounced for the latter.

4. Validation by comparison to FE estimate and to numerical bounds

For validation purposes, we provide two different comparisons. We first compare the obtained criteria (30) and (37) with FE limit-analysis results recently reported by [35]. The FE computations were conducted on hollow sphere subjected at its external boundary to homogeneous strain rate conditions. As in the theoretical model, axisymmetric strain rate loadings are considered such that: $\Sigma_{11} = \Sigma_{22} \neq 0$, $\Sigma_{33} \neq 0$ and $\Sigma_{ij} = 0$ for $i \neq j$. The porous solid is made up of an anisotropic aluminium alloy for which the parameters (reported in table 1) were experimentally obtained by [2]. The corresponding macroscopic yield surfaces are presented in Fig3(a) for $p = 0.01$ and Fig 3(b) for $p = 0.1$. It is observed that the pre-

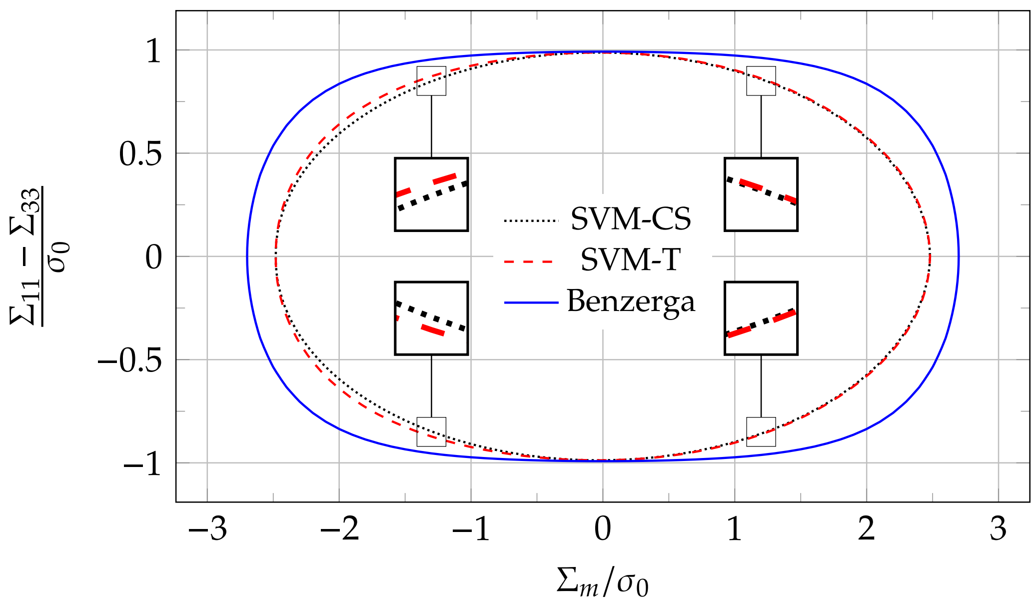

(a) porosity p=0.01

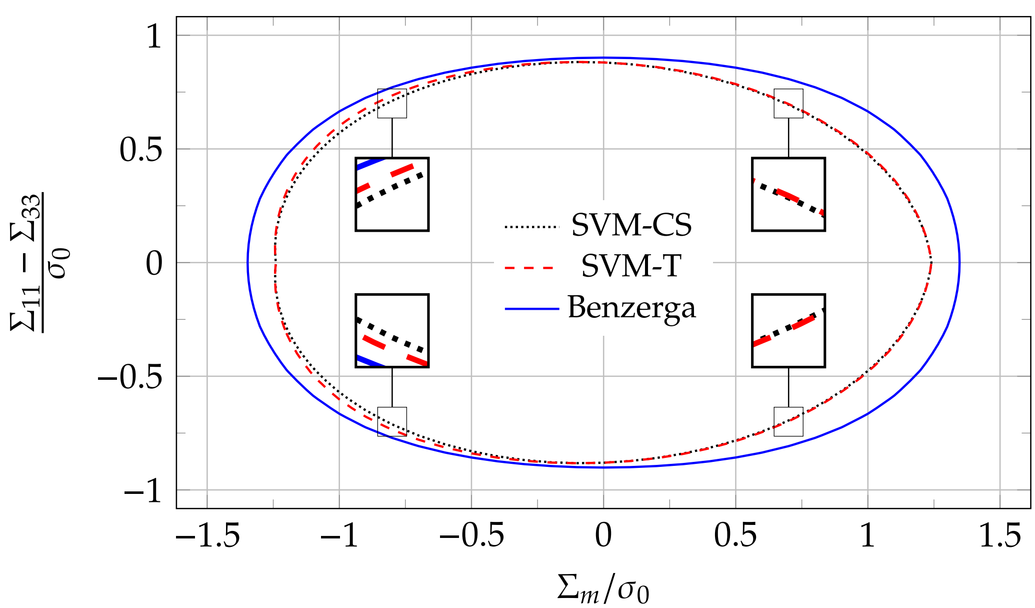

(b) porosity p=0.1

Figure 2: Hill matrix: comparaison of the yield surfaces given by the proposed new criteria given by eq (30) and eq(37) and that proposed by Benzerga et al. [4]

dicted envelope remains inside the yield envelopes obtained from the numerical FE results, as expected. However, one can note that the criterion obtained by [4], by using a kinematic approach provides closer upper bounds when compared to FE results. This fact may be explained by the fundamental difference between the kinematic and the static limit analysis approaches. More specifically, the difference with Benzerga criterion may be attributed to the relaxation of the yield condition in the matrix, this condition being enforced only in the mean and by assuming a uniform plastic multiplier. The same observation has been also made in the case of an isotropic matrix in [8].

A second assessment of the accuracy of the proposed criterion is performed by comparing the theoretical predictions to Pastor et al. [38] upper and lower bounds of the macroscopic criterion for anisotropic materials. Those bounds are obtained using respectively static and kinematic FE approaches and based on the solution to the corresponding conic programming problems[10]. In Fig 4 the yield surfaces projected in the plane ($\Sigma_{11} - \Sigma_{33}$, Σ_m) corresponding to the established criteria (30) and (37) are compared to the bounds given by the static and kinematic codes from [38]. In all quadrants, the theoretical criteria predict a macroscopic yield envelope inside the numerical lower bound. The discrepancy observed between the analytical model and the numerical results is probably due to the isotropic character of the used stress field which does not incorporate the anisotropy of the matrix. In particular, for hydrostatic loadings, the model does not predict the exact solution which can be estimated from the numerical upper and lower bounds. However, the accuracy is quite satisfactory when the stress triaxiality is low or moderate.

In summary, the assessment of the proposed model can be considered successful;

[10] *the readers interested by this original numerical approach and its application to various porous materials can refer to [37].*

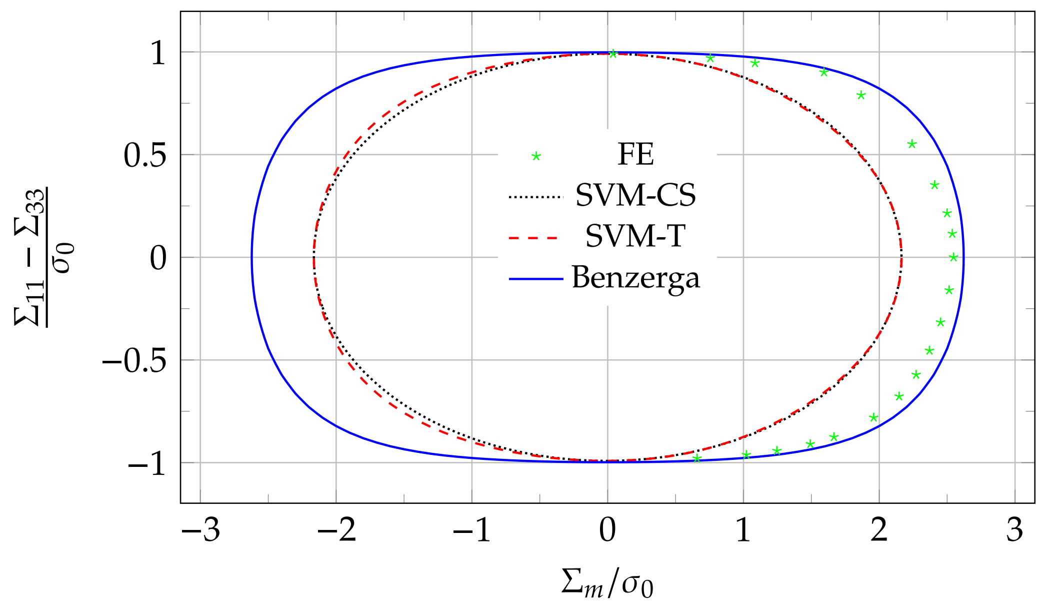

(a) porosity p=0.01

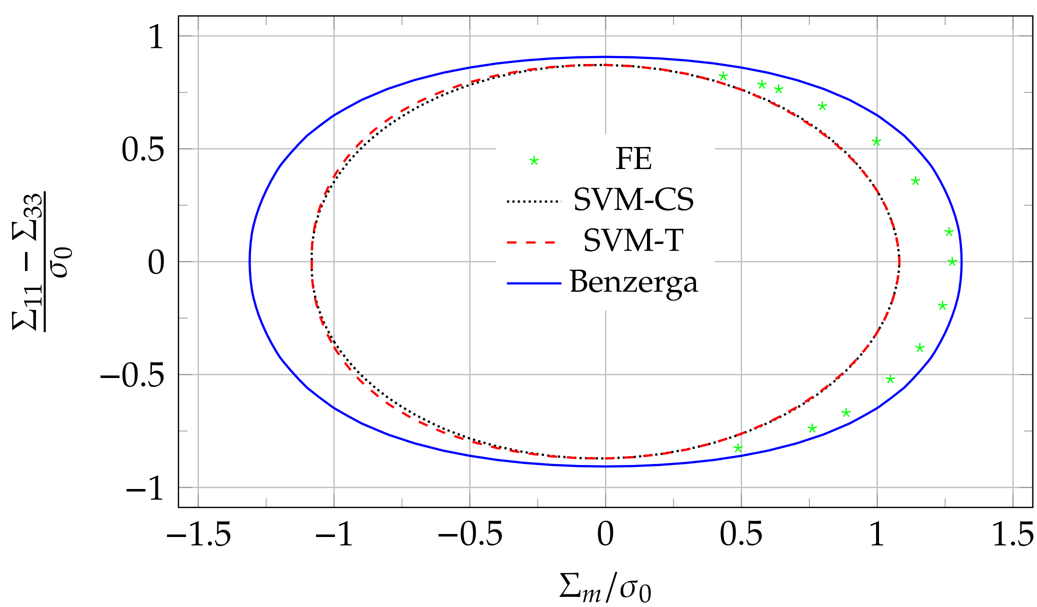

(b) porosity p=0.1

Figure 3: Hill matrix: comparaison of the yield surfaces given by the proposed new criterions eq(37)and eq(30) and by FE [35]

moreover it must be emphasized that, to the best of our knowledge, it is the first criterion which accounts for the effect of the sign of J_3 in a context of ductile porous materials with an anisotropic matrix.

5. Plastic flow rule and void growth

The macroscopic plastic flow rule is obtained from the normality law already presented in (14). The macroscopic mean and deviatoric parts of the plastic deformation are readily obtained in the form :

$$
\begin{aligned}
D_m &= \frac{1}{3}\dot{\lambda}\frac{\partial F}{\partial \Sigma_m} = \frac{\dot{\lambda}}{6}\frac{\dfrac{18\beta}{\ln p^2}\dfrac{\Sigma_m}{\sigma_0^2} - \dfrac{3\Sigma_e \gamma sign(J_3)}{\sigma_0^2\sqrt{3/2(F+G)}\ln p}}{A(\mathbf{\Sigma})}, \\
D_e &= \dot{\lambda}\frac{\partial F}{\partial \Sigma_e} = \frac{\dot{\lambda}}{2}\frac{\dfrac{2\alpha}{3/2(F+G)}\dfrac{\Sigma_e}{\sigma_0^2} - \dfrac{3\Sigma_m \gamma sign(J_3)}{\sigma_0^2\sqrt{3/2(F+G)}\ln p}}{A(\mathbf{\Sigma})}
\end{aligned}
\tag{40}
$$

in which have been introduced the following scalar quantity:

$$
A(\mathbf{\Sigma}) = \sqrt{\frac{\alpha}{\frac{3}{2}(F+G)}\left(\frac{\Sigma_e}{\sigma_0}\right)^2 - \frac{3\gamma sign(J_3)}{\sqrt{\frac{3}{2}(F+G)}\ln p}\frac{\Sigma_e}{\sigma_0}\frac{\Sigma_m}{\sigma_0} + 9\frac{\beta}{\ln p^2}\left(\frac{\Sigma_m}{\sigma_0}\right)^2}
$$

Similarly, considering the macroscopic criterion obtained by Taylor series expansion (37), the corresponding macroscopic strain rates take the form:

$$
\begin{aligned}
D_m = \frac{1}{3}\dot{\lambda}\Bigg[&\frac{\partial D}{\partial \Sigma_m} + \frac{\gamma}{2}sign(J_3)\left(\frac{\dfrac{\partial C}{\partial \Sigma_m}D - \dfrac{\partial D}{\partial \Sigma_m}C}{D^2}\right) - \frac{\xi}{8}\left(\frac{\dfrac{2CD\partial C}{\partial \Sigma_m} - 3C^2\dfrac{\partial D}{\partial \Sigma_m}}{D^4}\right) \\
&+ \frac{\chi}{16}sign(J_3)\left(\frac{3DC^2\dfrac{\partial C}{\partial \Sigma_m} - 5C^3\dfrac{\partial D}{\partial \Sigma_m}}{D^8}\right)\Bigg]
\end{aligned}
\tag{41}
$$

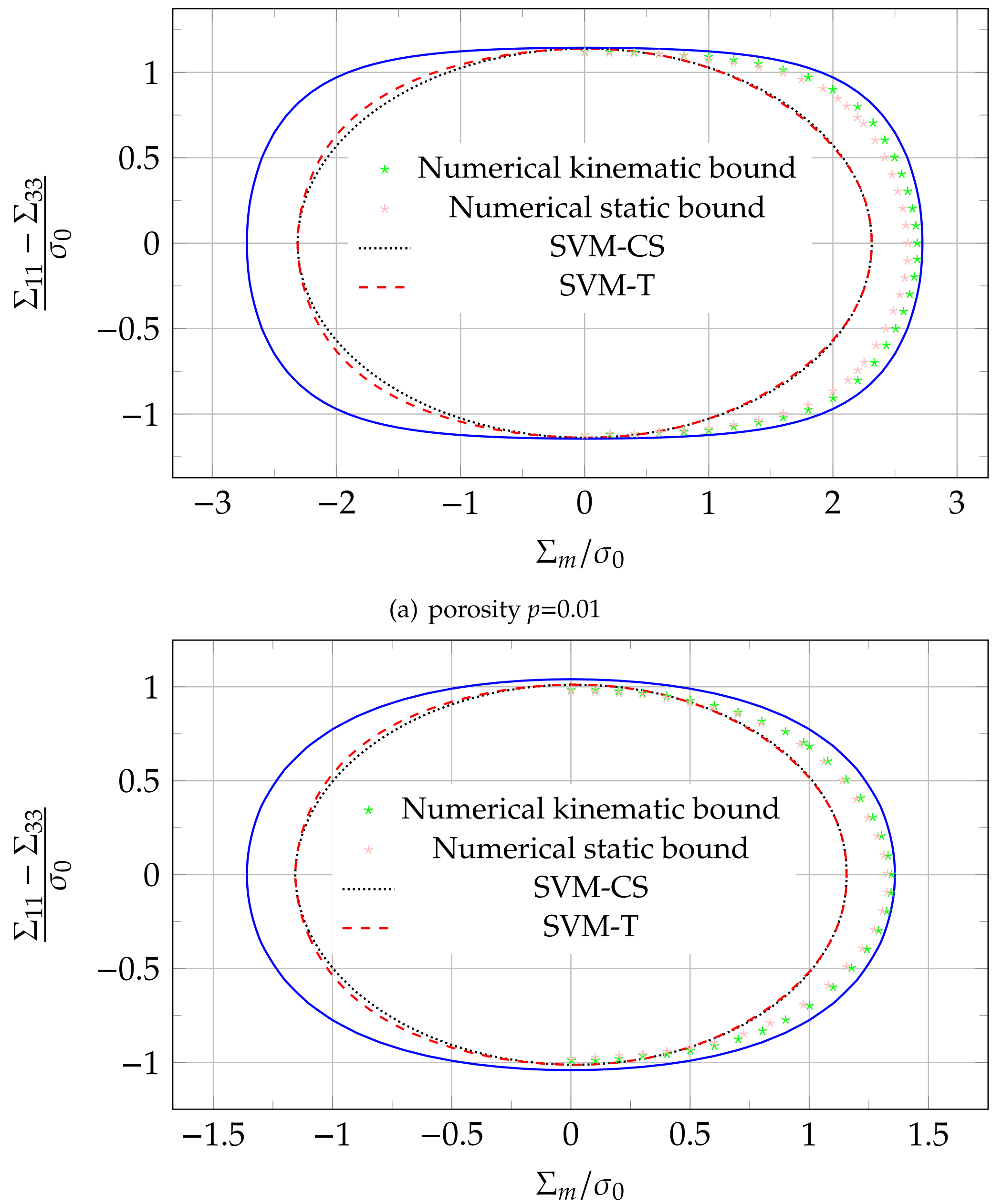

(a) porosity p=0.01

(b) porosity p=0.1

Figure 4: Comparison of the yield surfaces obtained from the established criteria (30) and (37) with numerical upper and lower bounds given by [38], porosity $p = 0.01$ and $p = 0.1$

$$D_e = \dot{\lambda}\Big[\frac{\partial D}{\partial \Sigma_e} + \frac{\gamma}{2} sign(J_3)(\frac{\frac{\partial C}{\partial \Sigma_e} D - \frac{\partial D}{\partial \Sigma_e} C}{D^2}) - \frac{\xi}{8}(\frac{\frac{2CD\partial C}{\partial \Sigma_e} - 3C^2 \frac{\partial D}{\partial \Sigma_e}}{D^4}) + \frac{\chi}{16} sign(J_3)(\frac{3DC^2 \frac{\partial C}{\partial \Sigma_e} - 5C^3 \frac{\partial D}{\partial \Sigma_e}}{D^8}) \Big] \tag{42}$$

in which have been introduced the following scalar quantities:

$$\begin{aligned}
&D(\mathbf{\Sigma}) = \sqrt{\alpha \tilde{\Sigma}_e^2 + \beta \tilde{\Sigma}_m^2} = \sqrt{\alpha(\frac{\Sigma_e}{\sqrt{3/2(F+G)}})^2 + \beta(-\frac{3\Sigma_m}{\ln p})^2}\,, \\
&\frac{\partial D}{\partial \Sigma_e} = \frac{\alpha \Sigma_e}{3/2(F+G)D}\,, \; \frac{\partial D}{\partial \Sigma_m} = \frac{9\beta \Sigma_m}{(\ln p)^2 D}, \\
&C(\mathbf{\Sigma}) = \tilde{\Sigma}_e \tilde{\Sigma}_m = -\frac{3\Sigma_m}{\ln p} \frac{\Sigma_e}{\sqrt{3/2(F+G)}}\,, \\
&\frac{\partial C}{\partial \Sigma_e} = -\frac{3\Sigma_m}{\ln p} \frac{1}{\sqrt{3/2(F+G)}}\,, \; \frac{\partial C}{\partial \Sigma_m} = -\frac{3}{\ln p} \frac{\Sigma_e}{\sqrt{3/2(F+G)}}.
\end{aligned} \tag{43}$$

Owing to the plastic incompressibility of the matrix, the porosity evolution is obtained from the mass balance equation, as in the case of the Gurson model:

$$\dot{p} = 3(1-p)D_m \tag{44}$$

The difference with the predictions of the Gurson model obviously lies in the dependence of D_m not only on the stress triaxiality but also on the characteristics of the anisotropic matrix as well as on the sign of the third stress invariant. Figs 5, 6, 7 and 8 illustrate the normalized evolution of porosity given as function of stress triaxiality for initial porosity $p = 0.01$ and different parameters of anisotropy. We consider the range [0..4] for T which corresponds to stress triaxiality levels for most commonly specimens used in ductile fracture experiments [3]. For completeness, these figures also include the predictions of Gurson [19] for the isotropic case and those of Benzerga et al. [4] model. The effect of the sign of the third invariant coupled to anisotropy parameters is much more pronounced for the porosity

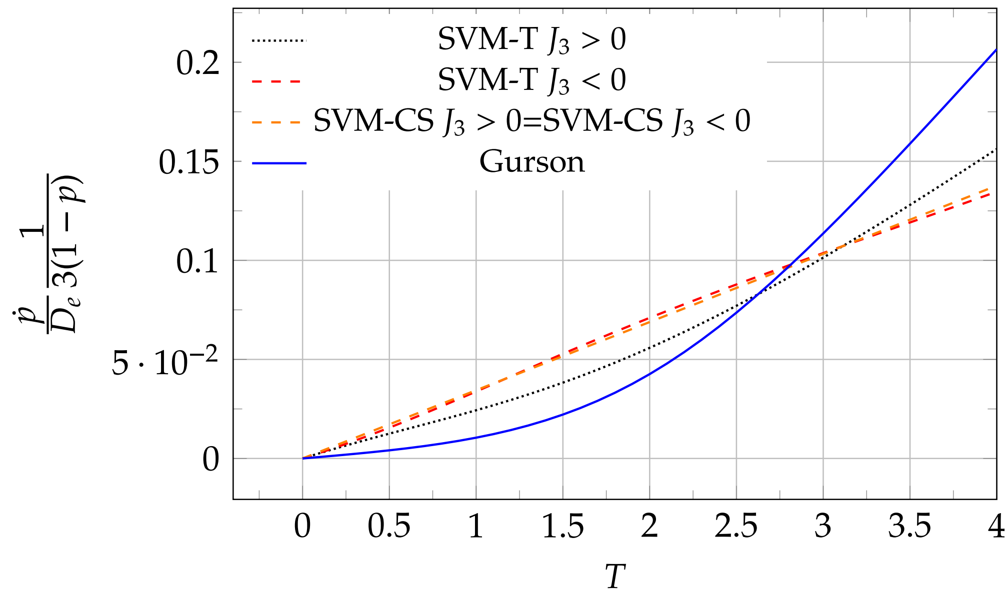

Figure 5: Evolution of porosity as function of the stress triaxiality for an isotropic matrix and for initial porosity p=0.01.

evolution than for the macroscopic criterion.

Conclusion

In this paper, we presented a new macroscopic yield criterion for plastic anisotropic materials obeying Hill's quadratic criterion and containing spherical voids. Specifically, this criterion is derived by generalizing to an anisotropic matrix the statical limit analysis approach recently proposed by Cheng et al. [8] for von Mises matrix. For the derivation of the macroscopic criterion, an appropriate statically admissible trial stress field has been considered. The obtained criteria are clearly impacted by the matrix anisotropy. A second interesting feature of the criterion obtained by a Taylor Series expansion is its dependence on the sign of the third invariant of the stress deviator, J_3, as well as on the two stress invariants Σ_m and Σ_e (Hill's equivalent stress). The criterion has been compared successfully to its theoretical kinematic counterpart proposed by Benzerga et al. [4] , to numerical data given by Pastor et al. [38] and to recent FE results of Morin et al. [35].

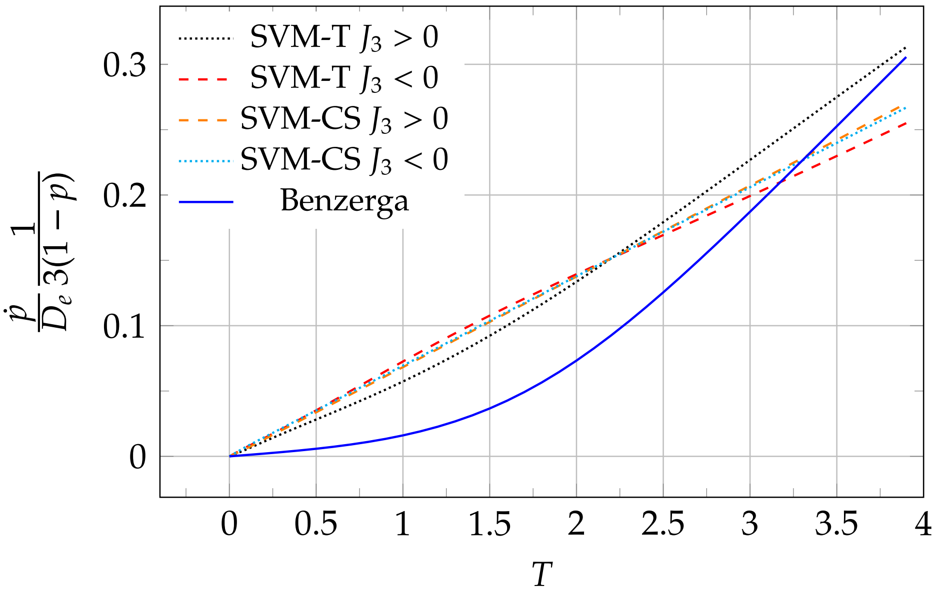

Figure 6: Evolution of porosity as function of the stress triaxiality for matrix parameters Set 2 in table 1 and for initial porosity p=0.01.

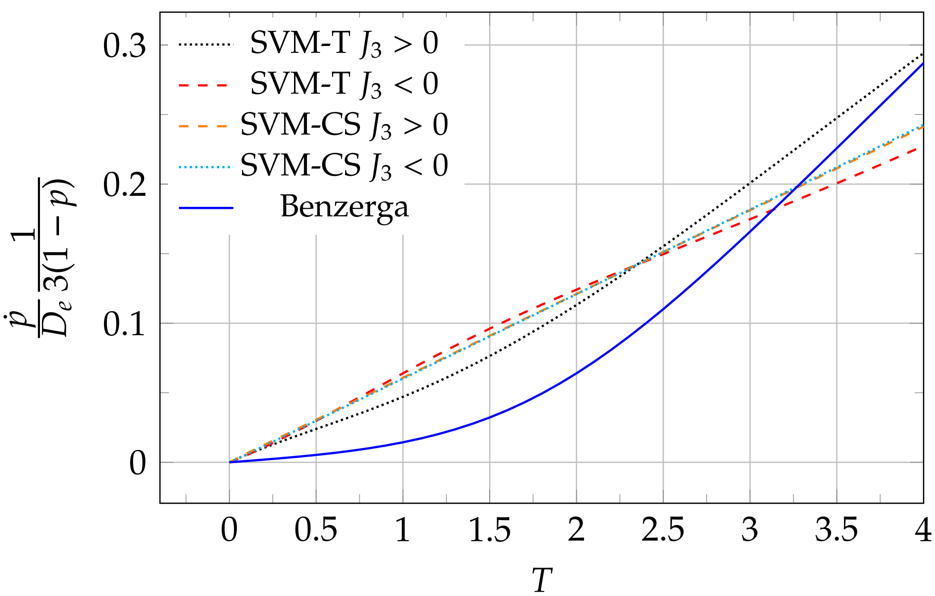

Figure 7: Evolution of porosity as function of the stress triaxiality for matrix parameters Set 3 in table 1 and for initial porosity p=0.01.

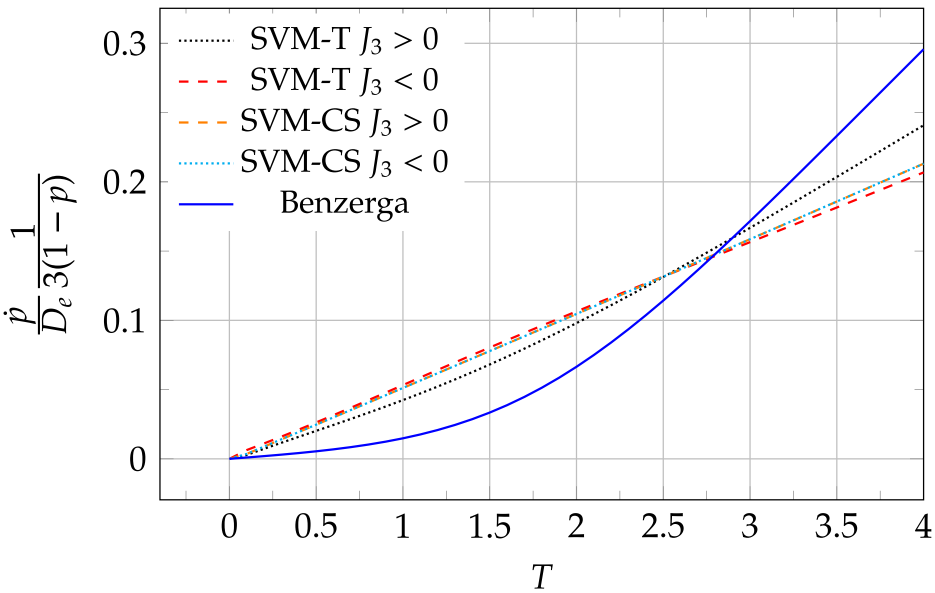

Figure 8: Evolution of porosity as function of the stress triaxiality for matrix parameters Set 1 in table 1 and for initial porosity p=0.01.

For completeness, we also provided the plastic strain rate equations and the void evolution law derived from the new criterion. It turns out that the effect of the sign of J_3 is more pronounced on the porosity evolution.

References

[1] Benallal, A., Desmorat, R., Fournage, M., 2014. An assessment of the role of the third stress invariant in the gurson approach for ductile fracture. European Journal of Mechanics - A/Solids 47, 400 – 414.
URL http://www.sciencedirect.com/science/article/pii/S099775381400028X

[2] Benzerga, A., 2000. Rupture ductile des tôles anisotropes. These de Doctorat, Ecole Nationale Supérieure des . . . .
URL http://scholar.google.com/scholar?hl=en\&btnG=Search\&q=intitle:Rupture+ductile+des+t\^{o}les+anisotropes\#0

[3] Benzerga, A., Leblond, J., 2010. Ductile fracture by void growth to coalescence. Advances in Applied Mechanics.
URL http://www.sciencedirect.com/science/article/pii/S006521561044003X

[4] Benzerga, A. A., Besson, J., May 2001. Plastic potentials for anisotropic porous solids. European Journal of Mechanics - A/Solids 20 (3), 397–434.
URL http://linkinghub.elsevier.com/retrieve/pii/S0997753801011470

[5] Castaneda, P., 1991. The effective mechanical properties of nonlinear isotropic composites. Journal of the Mechanics and Physics of Solids 39 (1), 45 – 71.
URL http://www.sciencedirect.com/science/article/pii/002250969190030R

[6] Castaneda, P. P., Suquet, P., 1997. Nonlinear composites. Vol. 34 of Advances in Applied Mechanics. Elsevier, pp. 171 – 302.

URL http://www.sciencedirect.com/science/article/pii/S0065215608703211

[7] Cazacu, O., Revil-Baudard, B., Lebensohn, R. a., Grjeu, M., Aug. 2013. On the Combined Effect of Pressure and Third Invariant on Yielding of Porous Solids With von Mises Matrix. Journal of Applied Mechanics 80 (6), 064501. URL http://appliedmechanics.asmedigitalcollection.asme.org/article.aspx?doi=10.1115/1.4024074

[8] Cheng, L., de Saxc, G., Kondo, D., 2014. A stress-based variational model for ductile porous materials. International Journal of Plasticity 55, 133 – 151. URL http://www.sciencedirect.com/science/article/pii/S0749641913001940

[9] Cheng, L., Guo, T., 2007. Void interaction and coalescence in polymeric materials. International Journal of Solids and Structures 44 (6), 1787 – 1808, physics and Mechanics of Advanced Materials. URL http://www.sciencedirect.com/science/article/pii/S0020768306003052

[10] Cheng, L., Monchiet, V., Morin, L., de Saxc, G., Kondo, D., 2015. An analytical lode angle dependent damage model for ductile porous materials. Engineering Fracture Mechanics 149, 119 – 133. URL http://www.sciencedirect.com/science/article/pii/S0013794415005548

[11] Chew, H., Guo, T., Cheng, L., 2006. Effects of pressure-sensitivity and plastic dilatancy on void growth and interaction. International Journal of Solids and Structures 43 (21), 6380 – 6397.

URL http://www.sciencedirect.com/science/article/pii/S0020768305005895

[12] Danas, K., Castaneda, P. P., 2012. Influence of the lode parameter and the stress triaxiality on the failure of elasto-plastic porous materials. International Journal of Solids and Structures 49 (1112), 1325 – 1342.
URL http://www.sciencedirect.com/science/article/pii/S0020768312000467

[13] Danas, K., Idiart, M., Castaneda, P. P., 2008. A homogenization-based constitutive model for isotropic viscoplastic porous media. International Journal of Solids and Structures 45 (1112), 3392 – 3409.
URL http://www.sciencedirect.com/science/article/pii/S0020768308000656

[14] Dang, N., Apr. 1976. Direct limit analysis via rigid-plastic finite elements. Computer Methods in Applied Mechanics and Engineering 8 (1), 81–116.
URL http://linkinghub.elsevier.com/retrieve/pii/0045782576900542

[15] GARAJEU, M., 1995. CONTRIBUTION A L'ETUDE DU COMPORTEMENT NON LINEAIRE DE MILIEUX POREUX AVEC OU SANS RENFORT.
URL https://books.google.be/books?id=HXnTMgEACAAJ

[16] Garajeu, M., Michel, J., Suquet, P., 2000. A micromechanical approach of damage in viscoplastic materials by evolution in size, shape and distribution of voids. Computer Methods in Applied Mechanics and Engineering 183 (34), 223 – 246.
URL http://www.sciencedirect.com/science/article/pii/S0045782599002200

[17] Gologanu, M., Leblond, J.-B., Perrin, G., Devaux, J., 1997. Recent Extensions of Gurson's Model for Porous Ductile Metals. Springer Vienna, Vienna, pp. 61–130.
URL http://dx.doi.org/10.1007/978-3-7091-2662-2_2

[18] Guo, T., Faleskog, J., Shih, C., Jun. 2008. Continuum modeling of a porous solid with pressure-sensitive dilatant matrix. Journal of the Mechanics and Physics of Solids 56 (6), 2188–2212.
URL http://linkinghub.elsevier.com/retrieve/pii/S0022509608000173

[19] Gurson, A., 1977. continium theory of ductile rupture by void nucleation and growth: Part I- yield criteria and flow rules for porous ductile media. Journal of Engineering Materials and Technology 99 (1), 2–15.

[20] Hill, R., 1948. A theory of the yielding and plastic flow of anisotropic metals. . . . of the Royal Society of London. Series A. . . . 193 (1033), 281–297.
URL http://rspa.royalsocietypublishing.org/content/193/1033/281.short

[21] Hill, R., 1950. The mathematical Theory of Plasticity.
URL http://onlinelibrary.wiley.com/doi/10.1002/9780470694626.ch6/summary

[22] Hill, R., 1967. The essential structure of constitutive laws for metal composites and polycrystals. J. Mech. Phys. Solids 17 (-), 79–95.
URL -

[23] Huang, Z., Yuan, X., Wang, R., Ning, J., 1996. Dynamic yield loci of a porous visco-plastic material by using a lower bound approach. IUTAM Symposia, 155–162.

URL http://link.springer.com/chapter/10.1007/978-4-431-65947-1_18

[24] J. Koplik, A. N., 1988. Void growth and coalescence in porous plastic solids. Int. J. Solids Structures 24 (-), 835–853.
URL -

[25] Jeong, H.-Y., 2002. A new yield function and a hydrostatic stress-controlled void nucleation model for porous solids with pressure-sensitive matrices. International Journal of Solids and Structures 39 (5), 1385 – 1403.
URL http://www.sciencedirect.com/science/article/pii/S0020768301002608

[26] Jeong, H.-Y., Pan, J., 1995. A macroscopic constitutive law for porous solids with pressure-sensitive matrices and its implications to plastic flow localization. International Journal of Solids and Structures 32 (24), 3669 – 3691.
URL http://www.sciencedirect.com/science/article/pii/002076839500009Y

[27] Keralavarma, S., a.a. Benzerga, Jun. 2010. A constitutive model for plastically anisotropic solids with non-spherical voids. Journal of the Mechanics and Physics of Solids 58 (6), 874–901.
URL http://linkinghub.elsevier.com/retrieve/pii/S0022509610000682

[28] Leblond, J.-B., Morin, L., Cazacu, O., 2014. An improved description of spherical void growth in plastic porous materials with finite porosities. Procedia Materials Science 3, 1232 – 1237.

URL http://www.sciencedirect.com/science/article/pii/S2211812814002016

[29] M.Gologanu, J., J.Devaux, 1993. Approximatemodelsforductilemetalscontaining non spherical voids - case of axisymmetric prolate ellipsoidal cavities. J. Mech. Phys. Solids 41, 1723–1754.

[30] M.Gologanu, J., J.Devaux, 1994. Approximatemodelsforductilemetalscontaining non spherical voids - case of axisymmetric oblate ellipsoidal cavities. ASME. J. Eng. Mater. Technol 116, 290–297.

[31] Michel, J., Suquet, P., 1992. The constitutive law of nonlinear viscous and porous materials. Journal of the Mechanics and Physics of Solids 40 (4), 783 – 812.
URL http://www.sciencedirect.com/science/article/pii/002250969290004L

[32] Monchiet, V., Cazacu, O., Charkaluk, E., Kondo, D., Jul. 2008. Macroscopic yield criteria for plastic anisotropic materials containing spheroidal voids. International Journal of Plasticity 24 (7), 1158–1189.
URL http://linkinghub.elsevier.com/retrieve/pii/S0749641907001210

[33] Monchiet, V., Charkaluk, E., Kondo, D., 2014. Macroscopic yield criteria for ductile materials containing spheroidal voids: An eshelby-like velocity fields approach. Mechanics of Materials 72, 1 – 18.
URL http://www.sciencedirect.com/science/article/pii/S016766361300080X

[34] Morin, L., Leblond, J.-B., Kondo, D., 2015. A gurson-type criterion for plastically anisotropic solids containing arbitrary ellipsoidal voids. International

Journal of Solids and Structures 77, 86 – 101.
URL http://www.sciencedirect.com/science/article/pii/S0020768315002395

[35] Morin, L., Madou, K., Leblond, J.-B., Kondo, D., Jan. 2014. A new technique for finite element limit-analysis of Hill materials, with an application to the assessment of criteria for anisotropic plastic porous solids. International Journal of Engineering Science 74, 65–79.
URL http://linkinghub.elsevier.com/retrieve/pii/S0020722513001250

[36] Pardoen, T., Hutchinson, J., 2000. An extended model for void growth and coalescence. Journal of the Mechanics and Physics of Solids 48 (12), 2467 – 2512.
URL http://www.sciencedirect.com/science/article/pii/S0022509600000193

[37] Pastor, F., Kondo, D., Pastor, J., 2013. 3d-fem formulations of limit analysis methods for porous pressure-sensitive materials. International Journal for Numerical Methods in Engineering 95 (10), 847–870.
URL http://dx.doi.org/10.1002/nme.4527

[38] Pastor, F., Pastor, J., Kondo, D., Mar. 2012. Limit analysis of hollow spheres or spheroids with Hill orthotropic matrix.
URL http://linkinghub.elsevier.com/retrieve/pii/S1631072111001975

[39] Perrin, G., 1992. Contribution à l'étude théorique et numérique de la rupture ductile des métaux. Ph.D. Thesis, Ecole Polytechnique.

[40] Perrin, G., Leblond, J. B., 1990. Analytical study of a hollow sphere made of plastic porous material and subjected to hydrostatic tension- application to some problems in ductile fracture of metals. Int. J. Plasticity 6, 677–699.

[41] Revil-Baudard, B., Cazacu, O., 2014. New three-dimensional strain-rate potentials for isotropic porous metals: Role of the plastic flow of the matrix. International Journal of Plasticity 60, 101 – 117.
URL http://www.sciencedirect.com/science/article/pii/S0749641914000746

[42] Save, M., Massonnet, C., de Saxce, G., 1997. Plastic limit analysis of plates, shells and disks.
URL http://books.google.com/books?hl=en\&lr=\&id=QRAtwWhycUoC\&oi=fnd\&pg=PP2\&dq=Plastic+limit+analysis+of+plates,+shells+and+disks\&ots=uvLN0muvWx\&sig=tBbNaxJpky-Glbh048yCA8ZF9O8http://books.google.com/books?hl=en\&lr=\&id=QRAtwWhycUoC\&oi=fnd\&pg=PP2\&dq=Plastic+limit+analysis+of+plates,+shells+and+disks\&ots=uvLN0muvWE\&sig=v5nJZYC_AaErtYx61wHKI7_1CGE

[43] V.Tvergaard, 1981. Influence of voids on shear band instabilities under plane strain conditions. Int. J. Frac 17, 389–407.

The author has requested enhancement of the downloaded file. All in-text references underlined in blue are linked to publications on ResearchGate.